

5110 0035

343

ITEM 35

TEXT + 10 LOOSE PLATES

"A PROGRESS REPORT ON THE GEOLOGY
& ORE DEPOSITS OF THE WARD
MINING DISTRICT, WHITE PINE
COUNTY, NEVADA"

SILVER KING MINES, INC.

by

TOM L HEIDRICK

FEB. 20, 1973

5110 0035

Phillips Petroleum Co.

343

ITEM 35

A PROGRESS REPORT ON THE
GEOLOGY AND ORE DEPOSITS OF THE WARD MINING DISTRICT
WHITE PINE COUNTY, NEVADA

SILVER KING MINES, INC.

by

Tom L. Heidrick

Tom L. Heidrick

February 20, 1973

TABLE OF CONTENTS

	Page
Introduction.....	1
Stratigraphy.....	1
Structure - Tectonics.....	8
Alteration-Mineralization and Ore Deposits.....	14
Ore Microscopy.....	27
Future Exploration and Development.....	35

FIGURES

Figure 1. Claim and section map.....	2 ✓
Figure 2. Generalized stratigraphy of Ward district.....	3 ✓ <i>don't have</i>
Figure 3. Geologic Map of the Ward district.....	5 ✓
Figure 4. Geologic-aeromagnetic map of Ward district.....	13 ✓
Figure 5a. Drill hole and mine map.....	17 ✓ <i>don't have</i>
Figure 5. Geologic-stratigraphic cross section A-A'.....	20 ✓ <i>don't have</i>
Figure 6. Geologic section A-A' showing ore zones.....	21 ✓ <i>don't have</i>
Figure 7. Composite altered-unaltered stratigraphic columns.....	23 ✓ <i>don't have</i>
Figure 8. Classification of sphalerite-chalcopyrite textures.....	28 ✓
Figure 9. Histogram of sphalerite-chalcopyrite textures.....	33 ✓
Figure 10. Geologic, aeromagnetic, and induced potential map.....	36 ✓ <i>don't have</i>
Figure 11. Map showing the geochemical distribution of copper.....	39 ✓

PHOTOMICROGRAPHS

Photomicrograph 1. Mixed sphalerite-chalcopyrite texture.....	29 ✓
Photomicrograph 2. Incipient unmixing of sphalerite-chalcopyrite...	29 ✓
Photomicrograph 3. Unmixing of chalcopyrite along fracture.....	30 ✓
Photomicrograph 4. Advanced unmixing texture.....	30 ✓
Photomicrograph 5. Unmixed-polarized texture.....	32 ✓
Photomicrograph 6. Unmixed texture.....	32 ✓

Introduction

The Ward mining district is located in east-central Nevada, 12 miles south of Ely in White Pine County. Ely is the largest city in this portion of Nevada and the railhead for the Nevada Northern Railroad. The district is reached from Ely by traveling southeast seven miles on U.S. Highway 50, then south seven miles on graveled County Road 46, then west four miles on a graded road. As shown in Figure 1, the district is covered by 751 patented and unpatented mining claims totaling about 13,000 acres.

Stratigraphy

The district straddles the NNW-trending Egan Range at elevation 7,000 to 11,000 feet. Over 16,000 feet of Paleozoic dolomite and limestone with subordinate amounts of shale, sandstone, and siltstone crop out within the district. Ordovician to Mississippian dolomite, limestone, shale, and sandstone dominate much of the terrain in the west while Pennsylvanian-Permian limestone and sandstone crop out in the eastern portion of the district. This sedimentary cover was subsequently intruded by middle Tertiary plutons, dikes, and sills of quartz monzonite, quartz monzonite porphyry, and finer grained equivalents. Comagmatic subvolcanic lithic and crystal tuffs vented along the range fronts feeding tuff sheets which crop out in the low foothills and underlie much of the flanking gravel pediments.

Figure 2 summarizes the Paleozoic and Tertiary stratigraphy of the district. This generalized column represents over 15,000 feet of stratigraphic sections measured within or immediately adjacent to the area shown in Figure 3. Excluding the Chainman Shale, all formations and members above the Middle Guilmette Limestone are indicated by representative lithologies as determined from either duplicate or triplicate measured sections. No sections were

measured prior to the completion of detailed mapping, nor were sections made in areas involved in structural complications or where poorly exposed. With the exception of the Sevy Dolomite, stratigraphy below the Guilmette Limestone is highly generalized and was constructed by integrating mapped lithologies with averaged stratigraphic thicknesses indicated by mapping (Figure 3).

Outcropping Ordovician, Silurian, and Devonian rocks within the Ward district and central Egan Range are characteristically miogeosynclinal in nature and suggest a rather gently subsiding shelf for a considerable span of geologic time. By Upper Guilmette time, however, the area began to show the first affects of the developing Antler orogenic belt to the west. Field work suggests that shelf conditions during this time were probably quite shallow and characterized by occasional emergent positive areas. Minor disconformable relations and rapid lateral facies changes within the sandy dolomite-dolomitic sandstone marker sequence of the Upper Guilmette Limestone, suggest that minor erosion occurred across these local emergent highs.

The contact between the Guilmette Limestone and overlying Pilot Shale is one of gradation involving a transition of 135-145 feet. The contact is placed above the last thin-to medium-bedded yellowish-brown weathering algal limestone and the first significant interbeds of platy-fissile calcareous shale. This break in lithology is everywhere quite distinct even though the basal calcareous shales of the Pilot often contain a few interbeds of silty-shaly algal limestone. This contact is readily picked in altered-mineralized drill core as well, since the last limestones of the transition zone are composed of discontinuous concentric masses of calcareous algae. In altered core, these algal masses show up as somewhat structureless spots and patches

which vary considerably in size and shape but which are repeatedly recognized.

The Cyrtospirifer-fauna of late Devonian age spans the Guilmette-Pilot contact, suggesting that the Devonian-Mississippian boundary lies well up within the Pilot Shale. The absence of fossils in the overlying black shales unfortunately makes it impossible to define the exact position of the boundary.

Duplicate sections measured at Rowe and Open Canyons indicate that the Upper Guilmette is 1,072 feet thick, while sections of the Pilot at Open, Efh, and Willow Canyons give an average thickness of 325 feet.

The early Mississippian Joana Limestone lies with apparent conformity upon the Pilot Shale and is overlain conformably by the Chainman Shale. The formation was measured at three different localities and found to vary in thickness from 362-455 feet. A minimum thickness of 360 feet is accepted for the district. The regional isopachous map for east-central Nevada demonstrates that this thickness is reasonable. Deposition of the Joana is believed to have occurred in restricted basins which were interconnected by shallow miogeosynclinal seas. In outcrop and in core, the formation is recognized by its light-gray color, crinoidal texture, or stratigraphic position (Figure 2).

The late Mississippian to early Pennsylvanian Chainman Shale forms a sage brush-covered strike valley that is continuously mantled by heavy black soil, talus, or colluvium. Often large areas of this bench are involved with Quaternary to Recent earthflow, debris flow, or extotic landslide blocks that have come down from the prominent Ely Limestone cliffs (Figure 3). Consequently, this poorly exposed interval was not measured in toto. Mapping demonstrates that there is 900-1000 feet of brownish mudstone and platy dark-gray to black fissile shale present in the lower portion of the formation; while the Scotty Wash Member consists of 300-350 feet of fine-to medium-grained quartz sandstone

and orthoquartzite intercalated with sandstone, siltstone and shale. The presence of laminated orthoquartzites, ripple marks, and cross-bedding suggest orogenically derived tongues of molasse shed from rising positive areas associated with the Antler orogenic belt. The marked variance in mapped thickness noted along strike is believed to reflect structural "squeezing" within this incompetent unit.

The contact between the Chainman and overlying Ely Limestone is gradational and is placed on the last occurrence of quartzitic sandstone or significant shale interbeds. Several sections of the Ely show the formation to be 2,500 feet thick. Limestone of the Ely is distinguished by its diagnostic faunal assemblages, varicolored chert zones, and variable lithology (Figure 2). In altered-mineralized portions of the district, the Ely-Chainman contact is placed on a sequence of spotted beds remanescant of those described earlier in the Pilot Shale. The spotted sequence is referred to as the "Caroline Beds" since they were first recognized in the deeper workings of the Caroline-Welcome Stranger mines. Most drill holes in the eastern portion of the district are collared above the Caroline Beds in Lower or Middle Ely Limestone. This portion of the Paleozoic section is of indirect economic significance since the high-grade Ag-Pb ores initially won from the Lower Ely are what gave the district its start in the 1860's.

In ascending order, the Permian rocks of the district include the Riepe Spring Limestone, Rib Hill Sandstone, and Arcturus Formation. The Pennsylvanian-Permian boundary, at the Ely-Riepe Spring contact, represents a regional disconformity throughout the Egan Range and is marked by a thin bed of dolomitic limestone conglomerate-breccia (Figure 2). Above the disconformity, the Riepe Spring is

a relatively chert-free coralline limestone measuring 225 feet in thickness. The Rib Hill Sandstone is 1125 feet thick with the lower 1/3 of the formation dominated by fossiliferous siltstone and sandstone that is calcareous and quartzose. The upper 2/3 of the Rib Hill consists of thin- to thick-bedded sandstone and siltstone with occasional intercalated beds of light-gray dolomitic limestone. The Arcturus Formation conformably overlies the Rib Hill and is approximately 3,000 feet thick elsewhere in the Egan Range. On a regional scale, the formation is divisible into a lower part of ledge-forming, medium-bedded fossiliferous limestone which rhythmically alternates with thin beds of silty sandstone; and an upper part dominated by thin-bedded platy, silty limestone, siltstone, and dolomite alternating with red to yellow weathering gypsiferous beds. In the Ward area, pre-Eocene erosion has removed most of the Upper Arcturus and only locally are mollusk-bearing gypsiferous beds preserved.

Unlike most of the pre-Chainman rocks of the Egan Range, most of the Pennsylvanian and Permian strata of the area contain appreciable amounts of sandstone, siltstone, and shale. This detrital material was shed eastward from the Antler orogenic belt and westward from highlands in west-central Utah. It was in the N-S trending trough between these two positive areas that clastics of the Ely, Rib Hill, and Arcturus were caught and preserved.

Denudation associated with the waning stages of the Antler orogeny and that associated with the late Cretaceous-early Tertiary Sevier orogeny, destroyed all records of post-Leonardian and Mesozoic strata in this portion of the Egan Range.

Scattered outcrops of lacustrine limestone overlie the Arcturus Formation along the east range front opposite the Ward district (Figure 3). These

Fresh-water limestones are equivalent to the Eocene Sheep Pass Formation which crops out sporadically throughout east-central Nevada. At Ward the formation is at least 350 feet thick and rests with angular unconformity upon the Arcturus Formation. The formation is readily subdivided into a lower member of siliceous conglomerate-breccia and an upper member of fine-grained bioclastic limestone containing diagnostic fresh-water mollusks and ostracods (Figure 2).

The Eocene lake beds are everywhere unconformably overlapped or intruded by extrusive-intrusive volcanic rocks. Figure 3 shows that the small volcanic field opposite the district consists of several composite vents delimited by centripetal flow layering showing maximum convergence polar to each respective throat. Petrographically and petrochemically these rocks are quartz latite in composition and possess textures indicative of lithic and crystal tuffs. The lithic tuffs contain numerous mineral fragments, accessory lithic fragments of previously consolidated volcanics, and accidental fragments derived from a subvolcanic basement of sandstone, siltstone, and limestone. The degree of vesiculation and welding varies considerably radially away from any given vent. Available field, petrochemical-spectrochemical, and K-Ar data strongly suggest that most tuff below the mid-Oligocene discontinuity (Figure 2) are temporal and chemical equivalents of the outcropping quartz latite porphyries (dikes, sills, intrusion breccias, and plug) of the district. Consanguinity between intrusive tuff and the porphyry mass that underlies most of the district is also inferred since K-Ar dating of biotite gives a 35 ± 1.3 m.y. age while normative and modal analyses yield quartz monzonite compositions. Little detailed petrography or petrology is completed on this mass, but it is clearly composite consisting of aplitic and "hybrid"

quartz monzonite porphyry or porphyritic equivalents. Most of the 40 drill holes penetrating the basal porphyry were terminated upon entering the mass and little detail is known concerning the areal distribution of the various facies. The thickness of the basal mass is unknown, but in the hole which penetrates the mass for over 1,000 feet, no appreciable textural or mineralogical changes are noted to this depth, suggesting that its total thickness is appreciable.

The subhorizontal welded ash flow tuff sheets overlying the mid-Oligocene disconformity appear identical to rocks outcropping in the Ward Charcoal Ovens area SSE of the district (Figures 2 and 3). K-Ar dating of the Ward Charcoal Ovens Tuff yields an age slightly younger than the early Oligocene intrusive rocks of the district.

The above data support the conclusion that all subvolcanic plutonism and comagmatic volcanism associated with the Ward volcanic center was completed in a short span of time. Emplacement involved no more than a few million years of early and middle Oligocene time which is temporally synchronous with many other volcanic and plutonic centers of the Great Basin. Similarly, drilling shows that the Cu-Zn-Pb-Ag mantos are spatially related to the basal porphyry, whereas mapping demonstrates that considerable silicification (limonitic and chert jasperoid) involve the Eocene Sheep Pass Formation and most of the intrusive-extrusive crystal and lithic tuff (Figures 2 and 3). The fact that silicification cuts the Eocene lake beds and siliceous leached caps overlie older lithic and crystal tuff, give congruency to the K-Ar dates and support the contention that sulfide mineralization at Ward is likewise genetically related to the early Oligocene

subvolcanic plutonism. The younger ash-flow tuff above the mid-Oligocene disconformity is interpreted as post-mineral and represents the final pulse of volcanism recorded in the district.

STRUCTURE - TECTONICS

The earliest and most intense deformation recorded in the Egan Range produced folds involving the entire Paleozoic sequence shown in Figure 2. During this period of deformation, eastward directed flow folding resulted in a major east-facing overturned asymmetrical syncline whose crestal plane cuts across Middle Ordovician thru Middle Permian strata. Fold axes associated with this period of deformation trend N10-20°W while associated crestal planes dip gently to moderately to the WSW. Low-angle thrust faults within the overturned limb of the syncline are recognized in all formations above the Chainman Shale. The pronounced thinning and structural deformation repeatedly noted in altered-mineralized Chainman reflect this oldest period of deformation. The age of the major overturned folding, thrusting, and bedding plane "shearing off" in the Chainman is not known with certainty. Indirect geologic reckoning suggests that the deformation is post-Permian and pre-Cenomanian in age. Known orogenies or disturbances which span this interval include the early Mesozoic disturbances of southern Nevada and either the Nevadan or Sevier orogenies. I personally prefer either of the two latter events.

Following the oldest period of deformation, this portion of the Egan Range experienced little or no recognizable Mesozoic deformation. Paleogeographic reconstructions of east-central Nevada show this area as

positive throughout most of the Jurassic and Cretaceous. This is structurally compatible with typical hinterland geology where local upwarps and broad open folds are the rule. By early Cenozoic time, however, hinterland "quiescence" had ended and local relief was the rule as implied by the limestone conglomerate-breccia found at the base of the Eocene Sheep Pass Formation (Figure 2).

The oldest post-Eocene high-angle normal and reverse faults strike N-NW parallel or subparallel to the present range front which they delimit. It was along these N-NW zones of weakness that the Ward dike swarm, composite intrusive tuff vents, and metallizing fluids were channeled upward to higher levels above the crystallizing basal porphyry. Synchronous with, as well as following this initial mid-Tertiary deformation, important normal faults, fault-veins, and veins formed in the transverse ENE direction. As shown by Figure 3, the transverse fracture zone as defined by detailed mapping of syntectonic veins, fault-veins, and faults, reaches a maximum width of 12,000 feet before its termination by NNW-trending Basin and Range faults. When studied in detail, the transverse fracture zone is seen to resemble a mosaic of horsts and grabens remanescent of those typically found over many elongate domes. As shown by Figure 4, the tectonic significance of this structural belt is emphasized once the district-wide aeromagnetic data are placed on top the geology of Figure 3. It is no coincidence that the transverse zone of deformation is precisely coaxial with the long dimension of the composite aeromagnetic high centered over the district. The marked correspondence between structure-tectonic and geophysical data takes on an air of economic significance when it is

realized that : 1) Over 95% of all outcropping intrusive and extrusive rocks of the district fall within the confines of the transverse belt or along its eastern projection; 2) Nearly all significant masses of metal-rich limonitic and cherty jasperoid fall within the transverse zone-exceptions being in those areas where major fracture zones cross the belt; 3) Multiple centers of intermineral subvolcanic plutonism break out where major NNW-trending Basin and Range faults intersect the eastern projection of the transverse zone; and 4) All known and drilled out deposits of the district are spatially restricted to the eastern most delineated horst of the belt. In light of these data, there is little doubt that the transverse zone represents syntaphrogenic fracturing and fissuring associated with NNW-SSE directed extension. Considerable differential elevation accompanied extension-distension as mirrored by the zone of axial horsts involving Ely Limestone and Chainman Shale. Flanking half-grabens are represented by the down-dropped Permian blocks south of the Ward Gulch fault and north of the Rowe Creek-Meadow Seep fault zones. It appears then that the motive force causing rifting is directly related to a magmagenetic process involving mid-Tertiary emplacement of the Ward intrusion. The configuration of this intrusion at depth is believed to conform in general with the aeromagnetic configuration shown in Figure 4. In cases of magnetic closure, we are most likely looking at a major discontinuity in the configuration of the porphyry-wallrock interface or marked changes in the magnetic susceptibility of involved rocks, or a combination of both these variables. As for the marked deterioration of the magnetic high in the eastern portion of the district, it is probably no coincidence that we find spatially associated with the area of steep negative gradient: 1) maximum structural deformation; 2) abundant

NW-trending porphyry dikes; 3) maximum development of metal-rich jasperoid; and 4) a proven site for contact-metasomatism and ore deposition.

Surface, underground, or diamond drill data clearly show the Ward Gulch and Meadow Seep-Rowe Creek half-grabens as active during as well as after emplacement of the porphyry dikes, crystal-lithic tuff vents, and sulfide-telluride mineralization. Likewise, the low-angle denudation faults mapped on the hanging wall of the half-grabens represent gravity propelled sliding concurrent with intrusion and resultant taphrogenesis. A mid-Tertiary synorotectonic age is requisite for this gravity sliding (denudation) since field data demonstrate that both bounding half-grabens and basal glide planes acted as conduits along which circulating hydrothermal fluids deposited metal-rich jasperoid in the Rowe Creek area and adjacent of strands of the east frontal fault system. As discussed later under Ore Deposits, reactivation of this fundamental framework continued throughout main stage contact metamorphism-metasomatism and served as important controls over ore localization and deposition. Post-mineral re-activation along many transverse and longitudinal elements has occurred repeatedly during Mio-Pliocene time and still continues today along the eastern range front.

In summary, if the geologic record at Ward has been deciphered correctly, all structures of the tectonic framework were established by the end of Oligocene time. Fold elements genetically related to Nevadan-Sevier deformation are dominated by N-NNW trends. Flexural Flow characterized this earliest deformation and minimal transverse and longitudinal fractured accompanied folding. Elements of Laramide age striking N-NW were activated prior to lacustrine conglomerate-breccia deposition of the Eocene Sheep Pass Formation, and may reflect "initial" collapse of the Great Basin province. Taphrogenesis

along the ENE-trending Rowe Creek-Ward Fracture zone commenced during early Oligocene time concurrent with emplacement of the buried Ward intrusion. By Oligocene time then, a simple pattern of faults, fissures, dikes, and vents was beginning to appear-one dominated by an orthogonal system striking E-ENE and N-NW. Continued re-activation of this fundamental framework during early Oligocene time had a marked influence on ore localization throughout this portion of the Egan Range. Following Oligocene plutonism, tectonism, volcanism, and ore deposition, Basin and Range faulting of Miocene age continued largely along pre-existing lines of structural weakness.

Historical Development of District

High-grade Ag-Pb ores were first discovered in the district in 1866. Between 1866 and 1885, production came from numerous small shafts and adits concentrated largely in the Good Luck and Caroline areas (Figure 5a). This early mining demonstrated that high-grade Pb-Ag ores were repeatedly localized as either: 1) small ill-defined shoots along dike contacts; or 2) crudely tabular mantos within the Caroline Beds. Both the Paymaster and Mountain Pride tunnels were driven during this era to further explore supposed downward extensions and continuations. No appreciable ore was discovered on either of these levels and the district received little further attention until after the turn of the century. Both the Paymaster and Mountain Pride tunnels were rehabilitated and extended in 1906 and 1927 respectively, but no discoveries were made. In the 1940's (Newmont Mining Company) and 1950's (Walker Corporation) extensive drifting and long-hole drilling were completed

From the Mountain Pride levels, again without making significant discoveries.

In 1962, Silver King Mines, Inc. was formed to further explore the district, and they initiated an extensive hammer-drilling program that demonstrated that significant deposits existed within the Caroline Beds immediately below both the Good Luck and Caroline areas. Underground exploration in the Welcome Stranger and Caroline mines was initiated in 1963, and open-pit mining started in the Caroline area in 1964. Ag-Pb-Zn ores were mined from the Caroline pit until 1966, when Phillips Petroleum Company obtained an option to acquire 51% of the Ward property.

Extensive shallow hammer-drilling completed in 1966 by Phillips, verified the presence of near-surface, low-grade Pb-Ag deposits immediately below the Good Luck area (Figure 5a). This deposit assays 6% lead and 3 ounces of silver and consists of plumbo-jarosite, cerrusite, anglesite, hemimorphite, and lesser amounts of other supergene products. Between 1967 and 1971, Phillips completed over 60 diamond drill holes averaging 1,500 feet in depth. Concurrent with much of this drilling, they re-opened the Mountain Pride tunnel and rehabilitated the Paymaster tunnel to its original length of 3,200 feet. Underground exploration from the Paymaster level involved driving the Defiance and Caroline crosscuts over 1,500 and 1,000 feet respectively. Mineralization encountered in the Joanna Limestone by the Defiance crosscut was further evaluated through longhole drilling and by driving several short crosscuts and raises.

The location of the underground workings and the collar position of the PW-series diamond drill holes are shown on Figure 5a. The depth, thickness, grade, and host rock for several significant ore intercepts are

summarized in the upper right hand corner of the figure. The line of Section A-A' corresponds to the geologic cross section shown in Figures 5 and 6. The bearing of structure contours used in projecting hole deviation and intercepts into A-A' are shown in plan by the dashed lines extending from each individual hole to the line of section. The bearing used in each instance was that pre-determined by structure contouring the Joana-Pilot contact.

Alteration-Mineralization and Ore Deposits

Within the area outlined by the JW-series (Figure 5a), about 40 holes penetrated the basal porphyry. The porphyry-wallrock contact is quite irregular in detail but overall conforms with the attitude of the overlying strata. This relationship is shown in some detail in section A-A' (Figure 5). As seen in this figure, the basal mass is penetrated at an average depth of 1800 feet with intercepts varying from a minimum depth of 1500 feet to a maximum of 2300 feet.

The dominant rock types and alteration-mineralization encountered in the basal porphyry are summarized in Figure 7. Hydrothermal alteration within the composite mass is commonly quite weak except for minor silicification along the wallrock contracts, and argillization-sericitization in areas of intense fissuring. Sulfide mineralization is largely restricted to either the occasional quartz veinlet and microfracture or within areas of intense fracturing-alteration. Disseminated pyrite, chalcopyrite, and molybdenite are ubiquitous but no intercepts to date have yielded significant ore-grade mineralization.

Most of the NW-trending dikes as seen in section A-A' extend to depth as near vertical structures. In many instances drilling demonstrates that

they extend well down into the basal porphyry before being lost. Sills of similar composition as the basal mass are common in the Chairman Shale and Lower Elly Limestone (Figure 5). The quartz latite and quartz monzonite porphyry dikes and sills are viewed as late stage differentiates of the basal intrusion. They invariably involved considerably more water during crystallization than did most of the basal mass as evidenced by their intense argillization-sericitization. Many of the high-level dikes and sills contain abundant amounts of disseminated pyrite and subordinate amounts of chalcopyrite and molybdenite; but only in the Good Luck and Caroline areas did the sills and dikes serve as favorable hosts for high-grade Ag-Pb ores.

The emplacement and subsequent cooling of the basal Ward intrusion caused widespread contact metamorphism, metasomatism, and marmorization of the supradjacent Paleozoic strata. The pronounced effects of this alteration-mineralization are appreciated when one compares unaltered and altered equivalent sections as is done in Figure 7. By viewing this figure in context with areal structure-tectonics, stratigraphy, and geophysics as well as cross sections 5 and 6, it is possible to arrive at several salient conclusions concerning the physicochemical controls of alteration-mineralization and ore deposition. A few of the more pertinent deductions are summarized below:

1. Each of the 10 diamond drill holes used in constructing Figures 5 and 6 encountered all respective formations, members, and sub-members in their proper stratigraphic position (Figures 5 and 7). In no instance are there two Pilot Shale intervals, or cases where Joana Limestone is stratigraphically lower or higher than its specified position, or where Dgs is present but no Dgt is logged. These data coupled with the geologic mapping (Figure 3) eliminate the possibility of multiple bedding-plane thrusts at Ward. Moreover, there is no stratigraphic or structural evidence which supports the contention that we crossed from a lower to upper thrust

plate in traversing from the drilled area to where the sections were measured - a matter of 3 to 5 miles. On the contrary, the presence of each Guilmette and Ely sub-member in its exact stratigraphic position, dictates the absence of plates at Ward. The extreme differential in stratigraphic thickness noted in Figures 5 and 7 must be explained by other means.

2. The altered-mineralized column of Figure 7 is correlated with strata deposited on a relatively stable miogeosynclinal shelf. The absence of recognizable unconformities, supratenuous folds, or significant facies changes within the mapped area (Figure 3), concurs with the suggested depositional environment. In this context, it is untenable to account for the observed stratigraphic thinning by any of the above processes.
3. The area of extensive drilling (Figure 5a) is located on the east-dipping homocline related to the Ward Mountain syncline (Figures 3 and 5). The geometry and internal features associated with folds throughout the district indicate a combination of mechanisms involving flexural flow and slip. Detailed stratigraphic sections of the Rib Hill Sandstone, Middle and Upper Ely Limestone, and Lower and Middle Arcturus were measured on the moderate to gentle, east-dipping homoclinal limb. All recorded thicknesses are comparable with those found on a regional basis. Differential flexural flow folding then cannot account for the extreme stratigraphic thinning of altered-mineralized sections (Figures 5 and 7).
4. The most feasible explanation for the enigmatic thinning which has perplexed so many, is one invoking non-volume-for-volume contact metamorphism-metasomatism-metallization associated with the emplacement and cooling of the Ward intrusion. This interpretation is strengthened repeatedly by observations such as those shown in section A-A'. In going up dip from PW-70 toward PW-35, one sees the Mj, MDp, Dgt, and Dgs thin differentially by 80%, 35%, 8%, and 60% respectively. When translated into an actual thinning with respect to unaltered Mj, MDp, Dgt, and Dgs (as shown in Figure 7) is 89%, 60%, 20%, and 69% respectively. Other sections pivoted about PW-35 show similar differential loss of section and demonstrate that the basal porphyry is dome-shaped with the cupola apex centered on the Upper Defiance area (Figure 5a).
5. It follows directly from 4, that there is indeed excellent stratigraphic continuity of altered-mineralized host rocks at Ward. Similarly, as shown in Figure 6, when the ore intercepts are placed on stratigraphic section A-A', it becomes clear that the orebodies at Ward are flat-lying, bedded deposits or stratabound mantos. Ores are selectively localized in metastratigraphic units at the top and bottom of the Joana Limestone, base of Dgt-top of Dgs, and at the interface between the contact metamorphic aureole and overlying

marble-skarn. The stratigraphic position, characteristic alteration-mineralization, and metal ratios are summarized for each important ore zone on Figure 7.

6. The porphyry contact is rather conformable with attitudes found in the overlying carapace, but in detail clearly cuts across the Dgs and Dgss. The apparent dips of stratabound deposits and metastrata shown in Figures 5 and 6 vary from 10-25° which corresponds to a true dip ranging from 16-45°. In this latter regard, all contacts were constructed by projecting corrected dips obtained from multiple attitudes measured in each cored interval. This procedure is believed to yield a more actualistic picture of stratigraphic-ore continuity than by merely connecting formational picks between adjacent holes.
7. Structural discontinuities are common in sections such as A-A' since they are drawn nearly perpendicular to the NW-trending lines of intense fracturing and diking within the central Ward block (Figure 3). In this respect, A-A' is viewed as representative of those sections showing maximum structural development. Near vertical normal and reverse faults as well as fault-veins are commonplace and appear related to abrupt perturbations in the basal porphyry contact. As for the NW-trending Paymaster-Good Luck dike set it is considered as essentially "rootless" (Figure 5). This is compatible with data obtained by drilling along their strike and by drifting-crosscutting under their projected downward extensions. It is suggested that this set of dikes is fed from either the east by the sill-like porphyry cutting PW-74, -67, and -78, or possibly from the west by conduits which apparently branch off from the steep, west-dipping Silver King dike. Synchronous with emplacement of the sill-like intrusions, activation along pre-existing NW-trending fractures plumbed the porphyry vertically through the competent overlying Ely Limestone. If this reconstruction is correct, we are no longer compelled to project this strong dike swarm to depth through one of the most important ore belts yet delineated by drilling.
8. Although there is no downward extension of the Good Luck-Paymaster porphyries, it is necessary to have an important structural discontinuity separating holes PW-60, -70, and -53 from PW-15, -78, and -63 (Figures 5a and 5). This fracture zone (Paymaster-Good Luck) served as channelways for heated skarn- and ore-forming fluids. Once through the Chaiman Shale blanket, the metal-rich fluids spread laterally in the Lower Ely Limestone producing massive epidote-clinzoisite-garnet skarn and depositing high-grade hessite-galena-sphalerite-chalcocite ores. More important, however, is the influence that the Good Luck-Paymaster fracture zone had on localizing Zn-Cu-Pb, Zn-Cu, Cu-Zn, and Cu mantos below the Chaiman cap. As seen on Figure 5a and in section A-A', the most important ores of the Joana and Guilmette occur within NW-trending belts flanking this feeder system. The succession of mantos from the Joana to the Guilmette transition ore zone, all appear

to have downward extensions "rooted" in this shear zone. Although no significant deposits are known within this near vertical fissure zone, this synthesis suggests that such deposits are likely - particularly where crossed by ENE-trending elements of the transverse zone.

9. After plotting the Upper and Lower Joana, Guilmette transition, and porphyry-Guilmette ore zones indicated on Figure 5a, the scarcity of ore holes west of the Silver King dike become quite obvious. This relationship is quite well-developed in section A-A', where each successive ore zone pinches out, terminates, or decreases appreciably in grade upon encountering or crossing the projection of the dike. The repeated duplication of this observation is more than fortuitous, and may reflect that the dike acted as a barrier to ore-forming fluids migrating up dip from the Paymaster-Good Luck feeders. This left the foreside strata cutoff from a ready source of metallizing liquors, which is mirrored today by the large barren area immediately west of the Silver King dike.
10. An intriguing deductive analogy of 9 appears in the explanation of the orebodies of the Caroline area (Figure 5a). Here the dikes or "barriers" continue to trend NW just as in the case of the Good Luck area. However in this instance, the dikes do not act as barriers since the Caroline area is located on the SSE dipping portion of the intrusive dome and altered-mineralized host rocks strike about N70°E. Consequently, the ore-forming fluids migrating in an up dip direction are traveling parallel to the plane of the Mammoth, Caroline, and Welcome Stranger dikes. The down dip feeder for the Caroline area turns out to be one of the largest intermineral structures yet recognized in the district - the Ward Gulch Fault (Figures 3 and 4). The barren core then is viewed as a direct magmatic consequence of doming by the Ward intrusion and emplacement of concomittant dike sets. Activation of cogenetic taphrogenetic structures coupled with differential metamorphism-metasomatism-stratigraphic thinning were critical physicochemical controls over ore localization, and all were spatially and genetically related to the emplacement-crystallization of the Ward intrusion.
11. The systematic succession of alteration-mineralization zones encountered with depth at Ward is likewise believed to represent a direct consequence of emplacement-crystallization of the basal porphyry. Progressive metamorphism-metasomatism grades from albite-epidote hornfels facies in the Ely Limestone and Chairman Shale to hornblende hornfels facies in the Mj, MDp, Dgt, Dgn, and Dgss on the flanks of the dome. Pyroxene hornfels are in general restricted to the immediate thermal contact metamorphic aureole. Details concerning individual assemblages are briefly summarized in Figure 7. Concurrent with the above changes in alteration, we experience sympathetic trends involving ore mineral suites commencing with hessite-calaverite-galena-pyrite-sphalerite in or above the Chairman, followed by sphalerite-chalcopyrite-galena-(pyrrhotite)-(tetrahedrite) in the upper and lower Joana ore zones, grading downward into pyrite-sphalerite-chalcopyrite-galena-tetrahedrite-chalcocite ores of the Guilmette transition, and finally magnetite-pyrrhotite-chalcopyrite-cubanite II-pyrite-bornite-enargite-molybdenite suites from the porphyry-

Guilmette ore zone. Details concerning Ag: Pb: Zn: Cu: Mo metal ratios and minor phases associated with this zoning pattern are summarized in Figure 7.

Ore Microscopy

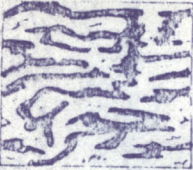
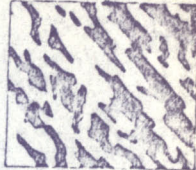
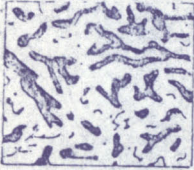
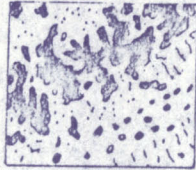
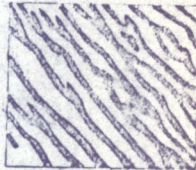
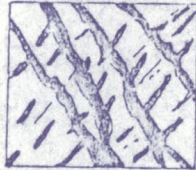




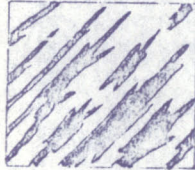


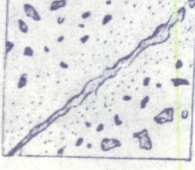


Since a great deal of literature exists which discusses the "typical" mineralographic nature and metallurgical problems encountered with chalcopyrite-sphalerite ores, this section briefly outlines several similar "atypical" relationships which exist in the Zn-Cu ores from the Ward district.

Over 100 polished and polished thin-sections have been made from metallized zones from the basal Porphyry, Guilmette, Pilot, Joana, and Ely formations. Figure 8 schematically summarizes the microtextures observed between coexisting sphalerite and chalcopyrite in these sections. All available observational data suggest that it is possible to group sphalerite-chalcopyrite intergrowths into four rather discrete classes as shown in Figure 8.


Microtextures of Class I or Mixed are dominated by uniform bead, uniform emulsion, and micrographic intergrowths of chalcopyrite within a sphalerite host (Photomicrograph 1). Chalcopyrite of Class I occurs as uniformly disseminated beads, rotund to scalloped blebs, or very fine-grained lamellae. The average size of exsolved chalcopyrite is quite variable but these preliminary investigations indicate that an average diameter of 10-20 microns or smaller is quite common.

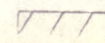
Class II or Initially Unmixed Microtextures are characterized by the general absence of uniform exsolution chalcopyrite throughout the sphalerite host, and by the coalescence of chalcopyrite blebs producing such non-uniform textures as submicrographic, sub-emulsion, and incipient syncrystic. Strong crystallographic control over the distribution and size of exsolved chalcopyrite is often apparent but the degree of such control varies from grain to grain as well as within individual grains. Where apparent, various combinations of chain, stringlet, and rod shaped intergrowths form along (001), (100), and (111) planes of sphalerite. Continued progressive unmixing causes initial Class II textures to grade imperceptibly into larger coherent segregation veinlets, lattice networks, or interpenetrant textures (Figure 8). Photomicrographs 2, 3, and 4 show the above sequential development of sphalerite-chalcopyrite textures through progressive subtypes of unmixing. Photomicrograph 2 depicts typical Class II mottled and sub-emulsion intergrowths. Here initial differential migration of Cu and Fe has left behind relatively large areas of "deined" sphalerite essentially free of Class I chalcopyrite. Photomicrograph 3 shows coarse-grained sphalerite host, but minor amounts of fine-grained Class I chalcopyrite. In this instance, the mobility of Class I Cu and Fe is believed to have been enhanced by the strain energy released along the microfault-vein that transversed the photograph from lower left to upper right. Under conditions of advanced

CLASSIFICATION OF SPALLERITE CHALCOPRITE TEXTURES
WARD DISTRICT, NEVADA

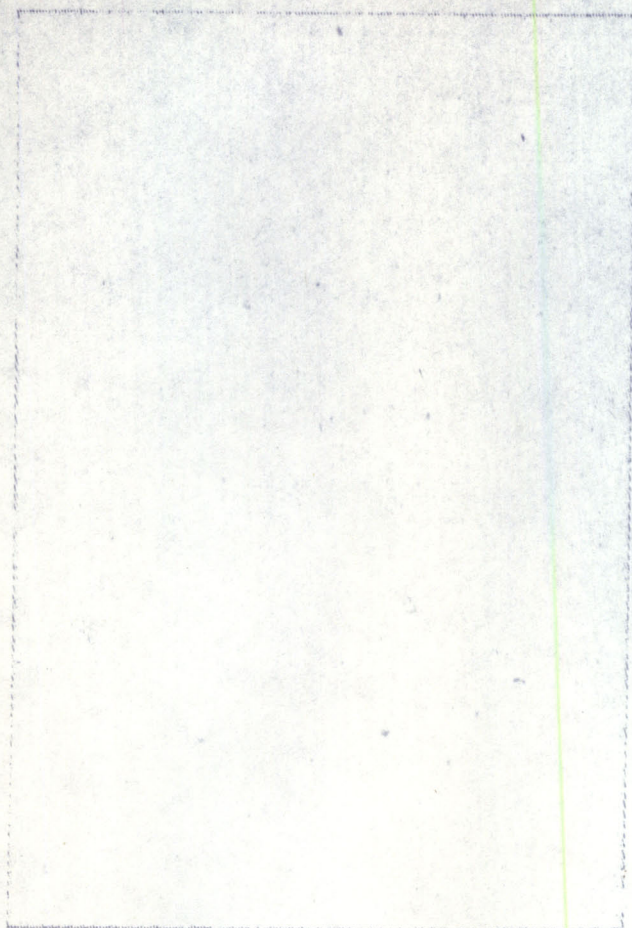
CLASS 1 MIXED	CLASS 2 INITIAL UNMIXING	CLASS 3 ADVANCED UNMIXING	CLASS 4 UNMIXED
 Factotum	 Submicrographic	 Adv. syncussis	 Braid
 Micrographic	 Sub-emulsion	 Segregation vein	 Band-ribbon
 Uniform emulsion	 Incip. syncussis	 Adv. interpenetrant	 Interstitial
 Uniform bead	 Lat. intergrowth	 Adv. rod and blade	 Ramifying veinlet
 Marginal zoning	 Interpenetrant	 Plume-flame	 Linear pseudoveins
 Arrested Diffusion	 Stringlet - rod	 Rotund - patch	 Fracture filling
	 Incip. seg. vein	 Perrinitic shred	 Rim-pind
	 Mix-Unmix breccia	 Polarized	 Peripheral bead

 Spallerite

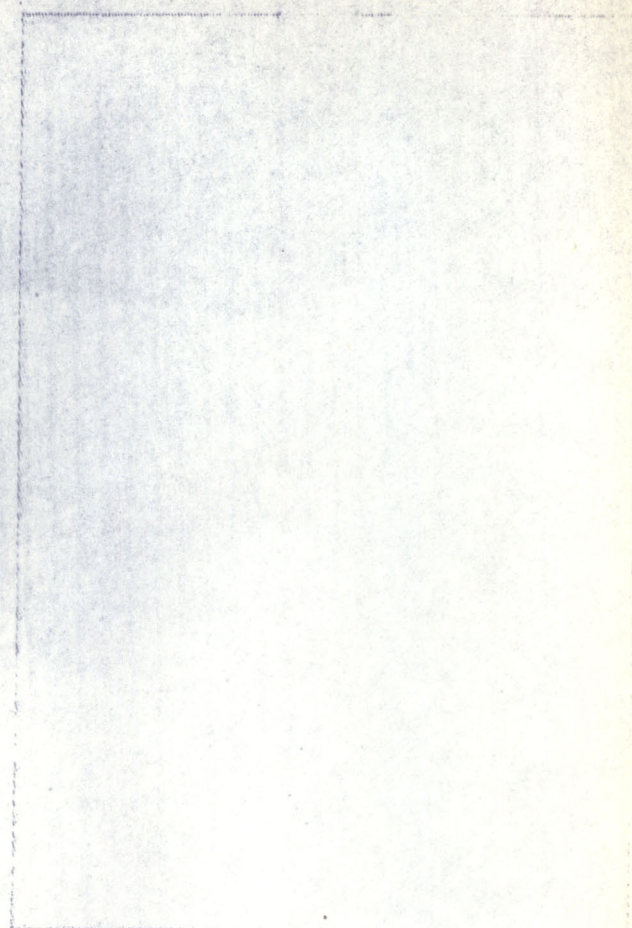
 Chalcopyrite

 Quartz

SPHALERITE - CHALCOPYRITE



Photomicrograph 1



Photomicrograph 2

0 300
Microns

Mixed to Incipient Unmixed sphalerite-chalcopyrite intergrowths. Sphalerite, chalcopyrite, and pyrite are grayish-brown, yellow, and white respectively.

Photomicrograph 1 exemplifies uniform bead-emulsion textures typical of the ore zones in the Ely, Joana, and occasionally the Upper Guilaette and Pilot. "Lanes" of unmixed sphalerite are believed to represent drained areas commonly observed marginal to sphalerite grain boundaries. In this instance, unmixing has occurred along natural sphalerite or sphalerite-chalcopyrite boundaries.

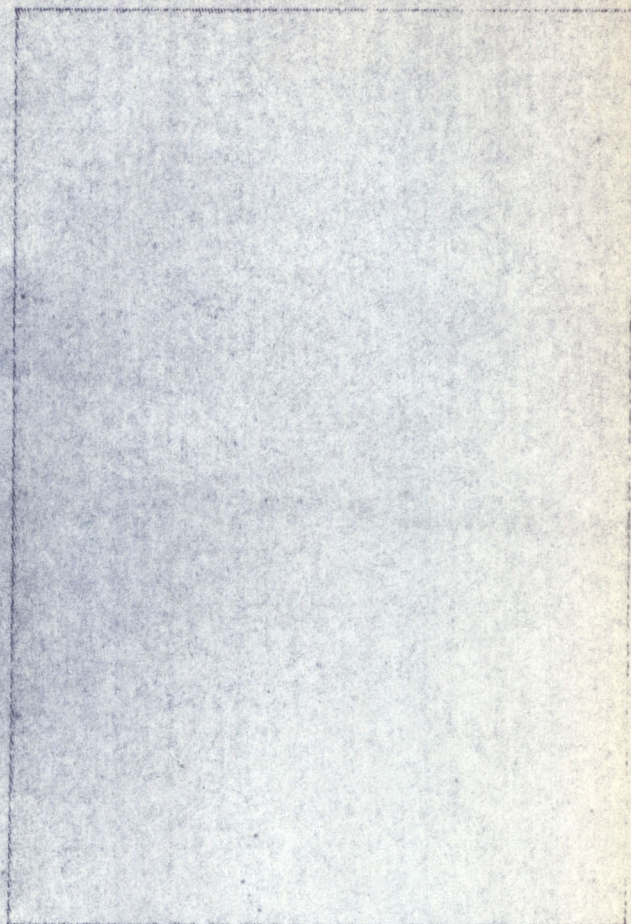
Photomicrograph 2 depicts typical Class II mottled and sub-emulsion chalcopyrite intergrowths in sphalerite. Drained areas within the sphalerite host are quite common in advanced stages of Incipient Unmixing. Drained areas such as that in the upper left apparently form in response to selective coalescing of smaller Class I chalcopyrite into larger than average blebs and lattice intergrowths as unmixing becomes progressively more advanced.

The bimodal distribution of exsolved chalcopyrite about frequency maxima 5-10 and 30-60 microns is well exemplified in both photomicrographs 1 and 2.

INCIPIENT AND ADVANCED UNMIXING
OF SPHALERITE - CHALCOPYRITE



Photomicrograph 3



Photomicrograph 4

0 1000
Microns

Incipient and Advanced Unmixing of sphalerite-chalcopryrite solid solution commonly observed in ores from the Upper Guilmette and occasionally in the Joana. Sphalerite, chalcopryrite, and pyrite are grayish-brown, yellow, and whitish-yellow respectively.

Photomicrograph 3 shows coarse-grained Class I sphalerite containing less than 2% by volume fine-grained Class I chalcopryrite. Draining of chalcopryrite from sphalerite apparently was enhanced by differential migration of Fe and Cu from supraadjacent sphalerite toward the microfault-vein which traverses the photograph from lower left to upper right. Should such structural deformation become penetrative at this scale, an ore fabric similar to that shown in Photomicrograph 4 might be expected. Here, advanced unmixing has resulted in large 100-200 micron lamellae surrounded by abundant 80-100 micron submicrographic intergrowths of chalcopryrite. Under conditions conducive to more advanced unmixing (continued deformation, higher temperatures, etc.) such peritectic lamellae and serrated shears continue to grow at the expense of Class I chalcopryrite resulting in a fabric dominated by wide 300-500 micron bands of sphalerite completely free of micrographic intergrowths.

progressive unmixing, large serrated exsolution lamellae and blebs of chalcopyrite continue to grow at the expense of smaller dispersed blebs. The resulting texture is one showing relatively large bands of sphalerite which are completely "drained" of 10-20 micron Class I chalcopyrite (Photomicrograph 3). Data concerned specifically with grain size distribution for Class II exsolved chalcopyrite is still incomplete, however, that at hand strongly suggests a trimodal distribution about frequency highs at 10-20, 70-120, and +240 microns.

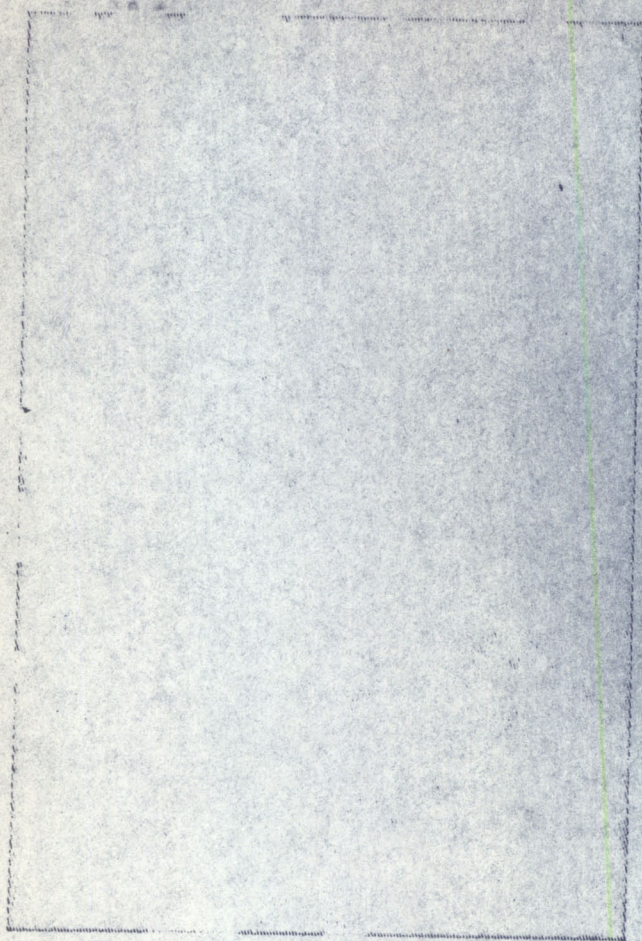
Class III or Advanced Unmixed textures are recognized by the progressive elimination of such fine-grained textures as incipient syncussis-stringlet, rod and incipient segregation veins by such textures as advanced syncussis, advanced rod-blade, and well developed segregation veins respectively (Figure 8). Photomicrograph 4 is representative of Class III unmixing where perrenitic shreds of chalcopyrite often measuring 200-300 microns are surrounded by abundant submicrographic intergrowths of chalcopyrite that measure 80-100 microns in maximum dimension.

The "polarization" of chalcopyrite in the center and/or peripheral to sphalerite is considered an advanced stage of Class III (Figure 8). Photomicrograph 5 depicts this tendency of chalcopyrite to occur as small 10-50 micron beads near the center of large sphalerite grains and peripherally as large discrete grains measuring +80 microns.

Class IV or Unmixed textures end the sequel of chalcopyrite-sphalerite unmixing in the Ward ores. This stage of exsolution shows chalcopyrite coexisting with sphalerite as discrete interstitial grains, linear to ramifying veinlets, or as penetrative bands, braids, or ribbons (Figure 8). The most ubiquitous texture characterizing this stage of unmixing is that shown in Photomicrograph 6. Such "interstitial" textures contain both sphalerite and chalcopyrite (\pm bornite) without microscopic evidence for mutual exsolution intergrowths. Essentially all sphalerite is barren of exsolved chalcopyrite while chalcopyrite occasionally contains starlike to skeletal-shaped crystals of exsolved sphalerite. To date only chalcopyrite from ores of the unmixed type are known to show this latter textural relationship with sphalerite. Other diagnostic textures of Class IV include chalcopyrite as beads or rinds peripheral to large sphalerite grains or linear pseudoveins and fillings "cross-cutting" sphalerite free of chalcopyrite of Classes I, II, or III.

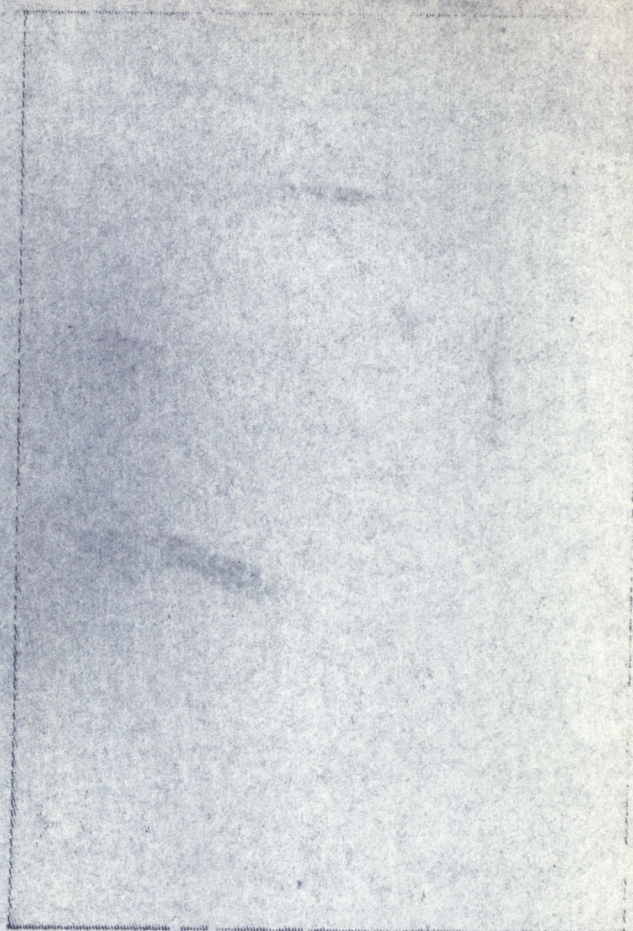
Vertical Zoning of Sphalerite-Chalcopyrite Textures.

The histogram of Figure 9 was constructed by first categorizing each polished section according to the fourfold classification outline above, and plotting each designated texture against their respective stratigraphic position. Where combinations of microtextures are the rule, they are plotted according to the scheme summarized in the explanation of Figure 9. A total of 84 sections contain adequate quantities of sphalerite and/or chalcopyrite to safely designate which class of unmixing is prevalent.



Photomicrograph 5

0 300
Microns



Photomicrograph 6

0 1000
Microns

Advanced to Unmixed sphalerite and chalcopyrite textures common to ores below the transition ore zone and within the basal porphyry. Sphalerite, chalcopyrite, pyrite, and bornite are gray, yellow, white, and mauve respectively.

Photomicrograph 5 shows the "polarization" of 5-10 micron blebs of chalcopyrite toward the center of a large interstitial grain of sphalerite. The larger 100+ micron grains of chalcopyrite situated peripheral to sphalerite appears to represent concomitant antipodal migration of Cu and Fe away from the chalcopyrite-rich core toward the margins of the host grain.

Photomicrograph 6 shows coarse-grained ores of coexisting sphalerite and chalcopyrite which are completely unmixed. All interstitial sphalerite is essentially free of all Class I and II chalcopyrite, while chalcopyrite often occurs intergrown with or closely associated to coexisting bornite, chalcocite, and pyrite. This unmixed texture is believed to represent the most advanced class of progressive destruction of Cu solid solution in sphalerite yet recognized in ores from the Ward district.

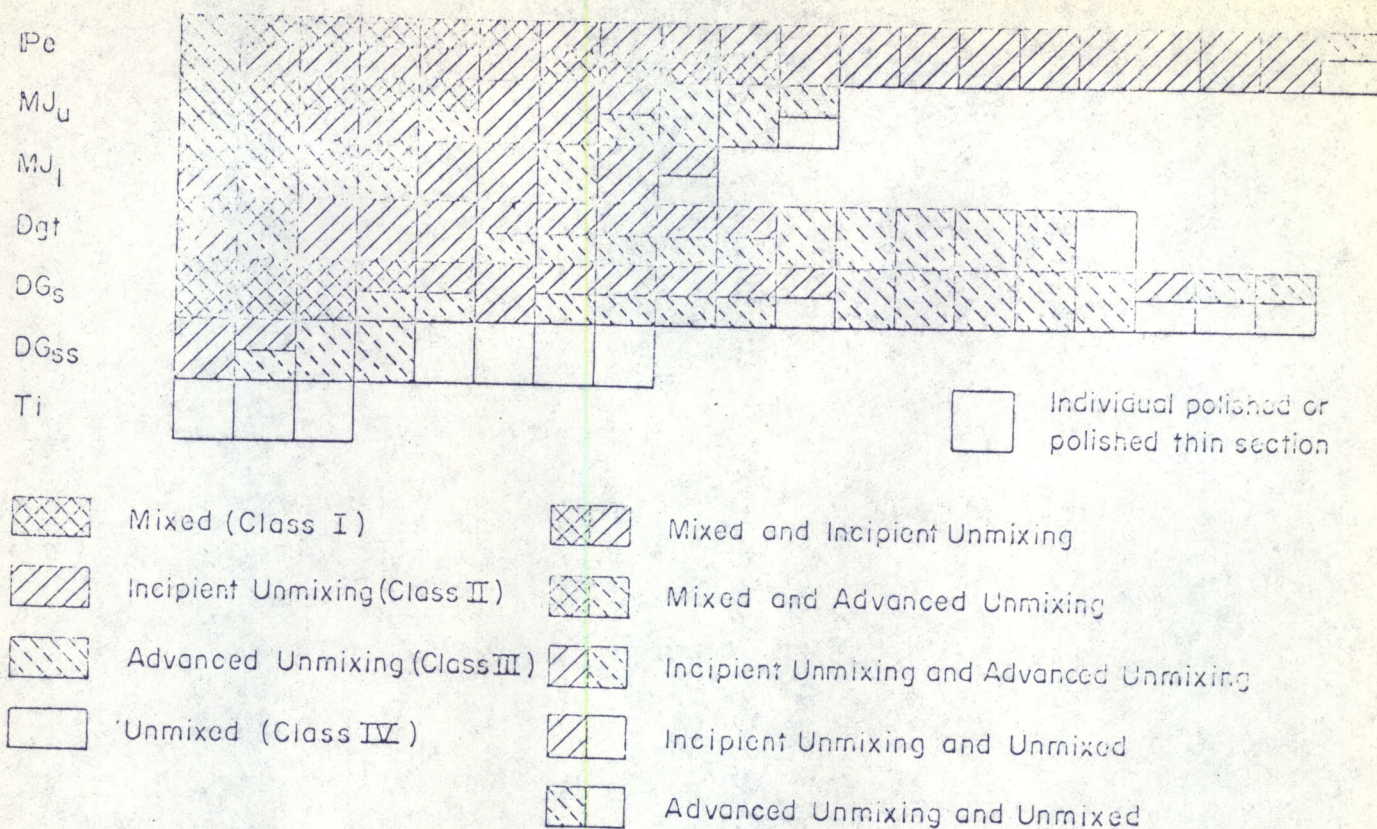


Figure 9. Histogram showing the distribution of sphalerite-chalcopyrite exsolution textures in stratabound ores from the Ward district, Nevada.

A comprehensive district-wide interpretation of Figures 8 and 9 is not feasible at this time since only 22 drill holes and 3 mines have yielded useable data concerning sphalerite-chalcopyrite unmixing textures. Moreover, the resulting frequency distribution per stratigraphic class interval shows a marked numeric bias toward the Ely and Guilmette limestones. Even with the above limitations, several pertinent and logical conclusions seem justified:

1. Unmixing textures characteristic of classes I thru IV are not randomly distributed between the various formations sampled.
2. Except for the Upper Joana ore zones, each class interval shows a marked internal textural consistency or bias. This internal coherence appears as textures dominated by combinations of classes I + II, classes II + III or classes III + IV.

3. Two grouped distributions also show marked internal textural consistency. Ores from the Upper and Lower Joana Limestone, and Ely Limestone represent the first group which are dominated by Class I and II textures while the second group of ores are pervaded by Class III and IV textures and come from ore zones in sub-members Dgt, Dgs, or Dgss.
4. The histogram of Figure 9 clearly demonstrates that ores from the basal porphyry (Ti) and Upper Guilmette Limestone (Dgss, Dgs, and Dgt) are dominated by Class III and IV textures and represent 100% of those specimens that are completely unmixed (U), 81% of those showing either U, or AU + U textures, and 83% of those that contain combinations of U, AU + U, or IU + U textures. On the other hand, those ore zones within the Joana and Lower Ely Limestone are dominated by Class I and II textures - 50% of all samples showing mixed (M) textures; 76% of those characterized by M, IU, and M + IU textures; and 66% of all ores exemplifying combination M + AU textures.
5. Preliminary microprobe analyses for Cu and Fe in coexisting chalcopyrite and sphalerite show chemical gradients that are sympathetic to observed textural changes. In the case of total dissolved Fe and Cu in sphalerite, ores from the Lower Ely typically contain no more than 1.75% Fe and no detectable Cu. With depth, however, sphalerite from the Joana contain 2.25% Fe and 0.25% Cu; while sphalerite from the Dgt and Dgs sub-members are distributed about two distinct populations - one with about 2.5-2.75% Fe and another with 8.5% Fe. Dissolved Cu in identical sphalerites from the Dgt and Dgs contain up to 0.5% Cu. The amount of total Cu in exsolved chalcopyrite is antipodal to the above gradients and decreases by over 1% with depth.
6. Data from 4 and 5 agree quite nicely with alteration-mineralization patterns discussed previously. The increase in metamorphic grade from epidote-albite to hornblende hornfels and sympathetic succession from telluride-galena-sphalerite to sphalerite-chalcopyrite-bornite-pyrrotite-magnetite ores suggest that the concurrent textural and chemical gradients are likewise intimately related to a marked increase in temperature of formation with depth. Sphalerite from the Ely and Joana therefore are believed to have formed at relatively low temperatures, were undersaturated with respect to both Fe and Cu and cooled (undercooled) relatively fast, yielding typical Class I and II textures. Sphalerite from the Guilmette sub-members experienced high temperatures of formation and cooled very slowly providing solute Cu and Fe the necessary ionic mobility to produce independent large grains outside the sphalerite host (Class IV textures).
7. These data on sphalerite-chalcopyrite textures at Ward concur with the common statement that chalcopyrite blebs, dots, and stringers are not randomly distributed throughout nature. They do not agree per se with the oft quoted postulate that chalcopyrite impregnations are most abundant in the contact-metamorphic deposits decreasing somewhat systematically to their

absence in the shallow-near surface deposits. On the contrary, Figure 9 shows a pronounced vertical zoning of sphalerite-chalcopyrite textures in Ward ores, and rather than possessing linear gradients of increasing chalcopyrite impregnations in sphalerite, we see ore dominated by unmixed textures with depth. For this reason, we believe that certain areas within Guilmette ore will not present the ubiquitous metallurgical problems encountered in "emulsion" ores like those from the Joana and higher stratigraphic units.

Future Exploration and Development

Copious geologic data concerning stratigraphy, structure-tectonics, alteration-mineralization, and geophysics in addition to thousands of assays and over 100,000 feet of core and cuttings are now available at Ward. This progress report represents an initial attempt to integrate some of the regional geology with the more detailed alteration-mineralization data obtained from drilling (Figure 5a). This synthesis clearly demonstrated the existence of a marked dependency between plutonism, tectonism, volcanism, and ore deposition within the district. The overall regional importance of the transverse ENE-trending Rowe Creek-Ward Fracture zone is mirrored by the coaxial distribution of cherty and limonitic jasperoid masses, dikes, and intermineral lithic and crystal tuff vents. On a smaller scale, we recognized similar genetic and spatial ties between doming by the band quartz monzonite and synchronous intensification of structure, alteration-mineralization, and steep negative aeromagnetic gradients in the drilled area (Figures 3, 4 and 5a). Many other gradients appear coincidental with entering the site of proven contact-metasomatism and ore deposition. In terms of future exploration and development the most important of these include data summarized in Figures 10 and 11.

Figure 10 shows the location of diamond drill holes and the position of four resistivity-induced potential traverses superimposed on the geology of the district. All induced potential lines were run independently by Powers, McPhar, and Hendricks on a maximum of 1,000 foot centers. In

plan these data define a somewhat linear zone of moderate to strong I.P. response trending subparallel to the Mammoth-Welcome Stranger-Defiance and Paymaster-Good Luck dike sets. Typically, this major anomaly is over 4000 feet wide, composite in detail, and extends from 1,500 to over 2,000 feet in depth without closure. All diamond drilling completed to date, except PW-74, falls within the major NW-trending anomaly; consequently, one cannot make a direct correlation between response and intensity of alteration-mineralization because every hole shows the affect of contact-metasomatism and metallization to some degree. What can be inferred, however, is the fact that alteration-mineralization of the type encountered in the PW-series holes extends well west of the Mammoth dike. In light of our earlier consideration of physicochemical controls and ore localization, the Mammoth dike may represent another "barrier" to ore-forming fluids migrating up-dip from the large normal faults mapped just west of the Upper Defiance area (Figures 3 and 5).

A geologic glimpse of what may lie beyond the drilled area west of the Mammoth dike is obtained by using PW-69 as a rotation axis about which A-A' is rotated 180°. After completing this operation, one obtains a mirror image of A-A', however, now the Mammoth plays the role of barrier dike - cutting off the foreside strata (barren core) from a ready source of ore-forming fluids. This situation then is viewed as analagous to the Silver King dike of section A-A' (Figure 6). Accepting this possibility, PW-75 takes on an air of importance being the first drill hole away from the Mammoth but within the area of strong I.P. response (Figures 5a and 10). It is significant to note that PW-72 is hammered to core point (Chinaman Shale) and its completion will shed much light as to what lies west of the dikes. Moreover, as shown in

Figure 6 (A-A') the ground west of the Mammoth is also readily accessible from the Defiance crosscut and relatively cheap underground drilling could be accomplished by extending this crosscut to the west beyond the dikes. Similar drilling from the Paymaster tunnel would also provide much needed information on grade and ore continuity in those mantos flanking the Good Luck fracture zone (Figures 5a and 6).

The only other significant I.P. response indicated on Figure 10 is restricted to the area immediately under or adjacent to the intrusive tuff vents. In this area the anomalies are quite shallow extending from a depth of less than 1,000 feet to well over 2,000 feet without closure.

Figure 11 summarizes the geochemical dispersion of copper as defined by over 200 plumbing samples of cherty and limonitic jasperoid, fault breccia-gouge, joint filling, and marmorized limestone. Regionally it is noted that rocks containing anomalous concentrations of copper are largely restricted to the transverse Rowe Creek - Ward fracture zone. On a more local scale, the areas of maximum Cu-dispersion occur as two rather linear belts parallel to the major dike sets of the district. The area between the two elongate highs is Cu-poor and is believed to reflect weak primary dispersion complimentary to alteration-mineralization of the barren core. The abundant shows of copper on the hanging wall of the Ward Gulch fault is interpreted as reflecting primary dispersion associated with the succession of footwall mantos delineated by drilling in the Caroline area (Figure 5a).

Unlike the I.P. anomaly which is open to the NW and SE (Figure 10), outcropping rocks containing high copper concentrations are much more restricted. Closure on the south appears spatially related to the trace of the Mammoth dike, while on the north closure occurs along Cu-bearing cross

fractures which trend ENE to W through the Upper Defiance area. Primary dispersion north of the Upper Defiance area stops rather abruptly and does not appear to reach the Meadow Seep fault zones. On the other hand, primary dispersion of copper south of the Ward Gulch fault suggest the possibility of down-dip extensions of the Caroline mantos to depths well below the last trace of Pennsylvanian footwall rocks.

Data concerning the dispersion of copper in the cherty and limonitic jasperoids associated with strands of the frontal fault system are not available at this time. However, in light of the Cu-content in similar jasperoids from the Rowe Creek area, it is suggested that the dispersion of copper does not terminate along the frontal faults, but actually extends well across the bounding faults (Figure 11). The common occurrence of indigenous limonitic boxwork in the intermineral intrusive-extrusive tuffs and innumerable masses of cherty and limonitic jasperoid in down-dropped blocks of Sheep Pass and Arcturus concur with this suggestion (Figures 3 and 11). The moderate I.P. response which underlies much of the area adjacent to the frontal faults (Figure 10) may be related to alteration-mineralization spatially associated with intense fracturing sympathetic to the frontal faults and emplacement of the intermineral intrusive tuffs. Considerable useful data concerning the nature of these intermineral intrusives and resulting alteration-mineralization are expected from PW-79 which is presently hammered to core point (Figure 5a).

In light of the foregoing discussion, it is apparent that much was accomplished by Phillips and Silver King during initial exploration of the district; but it is also apparent that much remains to be done. This is particularly the case in those extensive areas which remain unexplored for both manto-type deposits as well as disseminated-type deposits associated with the basal intrusive mass and intrusive-extrusive tuffs.

EXPLANATION

ALTERATION

STRUCTURE

LITHOLOGY

- Limestone
- Stromatolitic, cross-bedded
- Dolomite
- Sandy toward base
- Siltstone
- Limy, sandy and silty
- Shale
- Limy, sandy and silty
- Sandstone
- Quartzitic at base
- Chert
- Black bedded and semi-bedded
- Nodular and irregular
- Marble
- Marble breccia
- Albite-epidote hornfels
- Garnet-dioptase-epidote skarn
- Wollastonite-garnet-dioptase skarn
- Contact metamorphic aureole
- Andradite-wollastonite-dioptase skarn
- Siliceous intrusion breccia
- Silica breccia
- Collapse structures und.
- Mesoscopic drag fold
- Gravity fault
- Bedding
- Chaos

0 200 400 600
APPROXIMATE VERTICAL SCALE

Caroline Good Luck Ore Zone
Crude tabular mantos and small ill-defined cylindrical pods of high-grade ore localized along fault zones and dike contacts. All orebodies are found within garnet-epidote-clinozoisite-dioptase skarn. Ores contain appreciable amounts of pyrite, galena, sphalerite, pyrrhotite, hematite and chalcopyrite accompanied by subordinate amounts of calaverite, empressite, and stuetzite. Assayed metal ratios for Ag (oz): Pb (oz): Zn (oz): Cu (oz): Mo (oz) are 8:8:8:1:0.

Carbonaceous shale crosscut by numerous calcite-quartz veins dominate areas bordering the zone of intense alteration-mineralization. Within and peripheral to the barren core and mineralized areas epidote-chlorite-plagioclase-aegirine hornfels pervades the entire section. No significant ore intercepts known.

Upper and lower Joana Ore Zones

Upper limestone that is everywhere either metamorphosed, metasomatized, or silicified. Jasperoid, jasperoid breccia, and skarn occur as selective replacements along the bounding shale-limestone contacts. Skarn assemblages involve green andradite, gray diopside, wollastonite, and plagioclase. Ores consisting of pyrite, sphalerite, chalcopyrite, and galena with lesser amounts of pyrrhotite, tetrahedrite and petzite occur as mantos localized within the zones of jasperoid breccia and skarn. The upper ore zone is generally ill-defined and irregular while the lower zone shows much greater ore continuity. Assayed metal ratios for Ag (oz): Pb (oz): Zn (oz): Cu (oz): Mo (oz) for the upper and lower ore zones are 1.9:1.3:1.9:1.0 and 1.1:0.5:3.0:1.0 respectively.

Guilmette Transition Ore Zone

Mantos within either brown-green andradite-wollastonite-vesuvianite-thalite skarns after shaly-silty Dgt or within the silicified marble breccia at the top of Dgs. The mineralogy consists of pyrite, sphalerite, chalcopyrite, galena, tetrahedrite, and chalcocite with lesser amounts of enargite, cuprite II, pyrrhotite, hematite, covellite, and marcasite. Assayed metal ratios for Ag (oz): Pb (oz): Zn (oz): Cu (oz): Mo (oz) are 0.8:0.1:1.8:1.0.

Porphyry and fracture ore zone
Contact metamorphic aureole consisting of massive brown amphibolite, green diopside, wollastonite, sphalerite, and quartz. Ore zones occur either within this aureole (PW-67) or at its interface with overlying marble breccia (PW-75) characteristic ore mineralogy is relatively simple consisting of magnetite, pyrrhotite, chalcopyrite, cuprite II, pyrite, bornite, enargite, sphalerite, and wolframite. Assayed metal ratios for Ag (oz): Pb (oz): Zn (oz): Cu (oz): Mo (oz) are 0.5:0.1:0.1:1.0:0.3.

Composite aplite biotite quartz monzonite porphyry, porphyritic biotite quartz monzonite, and "breccia" quartz monzonite porphyry showing weak propylitic to phyllic alteration. Disseminated pyrite and chalcopyrite common. Microfractures and veins contain minor amounts of pyrite, chalcopyrite, molybdenite, sphalerite, and bornite. No significant ore intercepts noted to date.

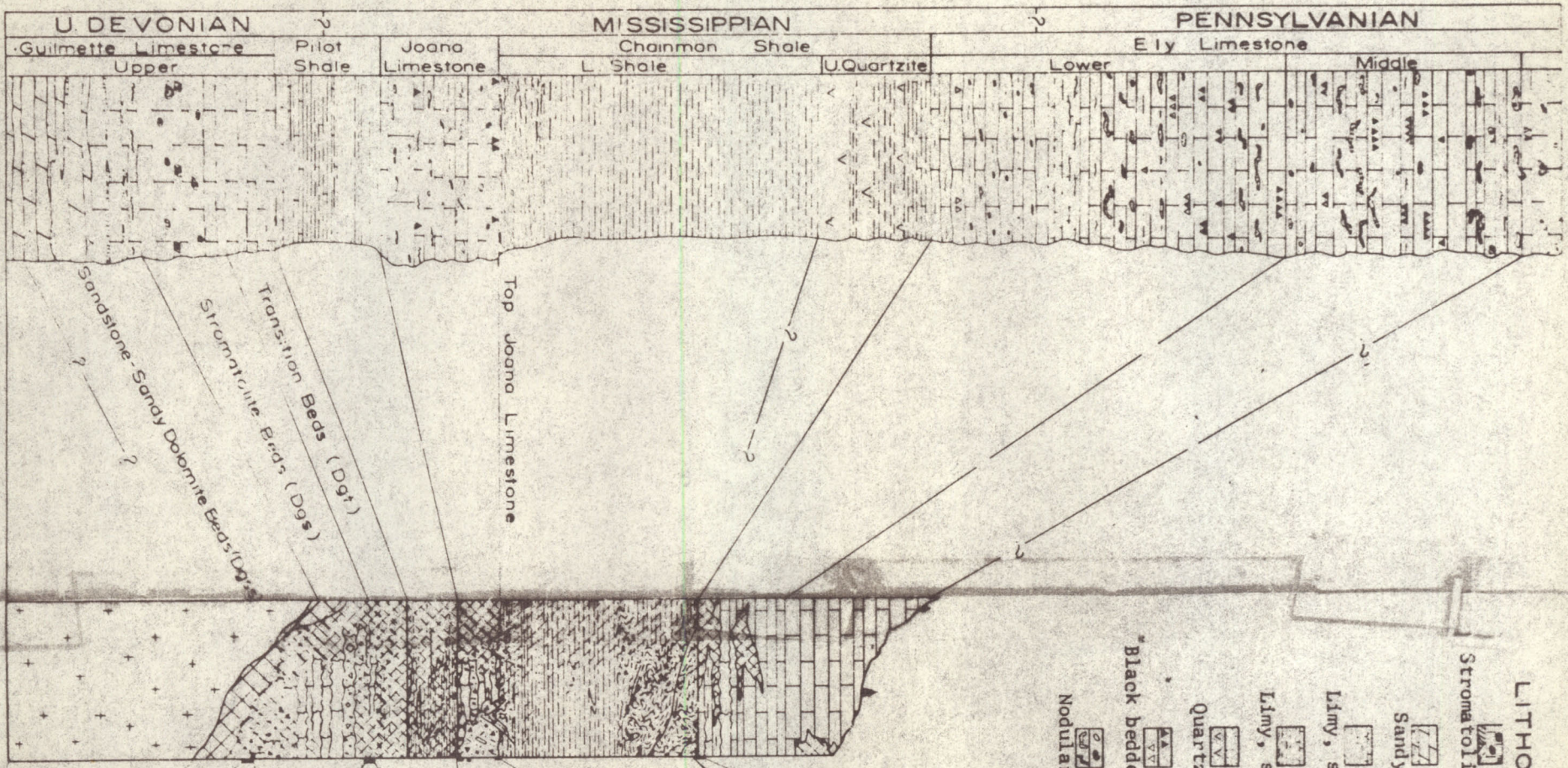


Figure 7. Composite stratigraphic sections showing unaltered and altered-mineralized equivalents, Ward District, Nevada.

EXPLANATION

ALTERATION

STRUCTURE

LITHOLOGY

- Limestone
- Stromatolitic, cross-bedded
- Dolomite
- Sandy toward base
- Siltstone
- Limy, sandy and silty
- Shale
- Limy, sandy and silty
- Sandstone
- Quartzitic at base
- Chert
- Black bedded and semi-bedded
- Nodular and irregular
- Marble
- Marble breccia
- Albite-epidote hornfels
- Garnet-diopside-epidote skarn
- Wollastonite-garnet-diopside skarn
- Contact metamorphic aureole
- Andradite-wollastonite-diopside skarn
- Siliceous intrusion breccia
- Silica breccia
- Collapse structures und.
- Mesoscopic drag fold
- Gravity fault
- Bedding
- Chaos

0 200 400 600
APPROXIMATE VERTICAL SCALE

Caroline Good Luck Ore Zone
Crude tabular mantos and small ill-defined cylindrical pods of high-grade ore localized along fault zones and dike contacts. All orebodies are found within garnet-epidote-clinzoisite-diopside skarn. Ores contain appreciable amounts of pyrite, galena, sphalerite, pyrrhotite, hematite and chalcopyrite accompanied by subordinate amounts of calaverite, empressite, and stuetzite. Assayed metal ratios for Ag (oz): Pb (oz): Zn (oz): Cu (oz): Mo (oz) are 8:8:8:1:0.

Carbonaceous shale crosscut by numerous calcite-quartz veins dominate areas bordering the zone of intense alteration-mineralization. Within and peripheral to the barren core and mineralized areas epidote-chlorite-plagioclase-aegirine hornfels pervades the entire section. No significant ore intercepts known.

Upper and lower Joana Ore Zones

Upper limestone that is everywhere either metamorphosed, metasomatized, or silicified. Jasperoid, jasperoid breccia, and skarn occur as selective replacements along the bounding shale-limestone contacts. Skarn assemblages involve green andradite, gray diopside, wollastonite, and plagioclase. Ores consisting of pyrite, sphalerite, chalcopyrite, and galena with lesser amounts of pyrrhotite, tetrahedrite and petzite occur as mantos localized within the zones of jasperoid breccia and skarn. The upper ore zone is generally ill-defined and irregular while the lower zone shows much greater ore continuity. Assayed metal ratios for Ag (oz): Pb (oz): Zn (oz): Cu (oz): Mo (oz) for the upper and lower ore zones are 1.9:1.3:1.9:1.0 and 1.1:0.5:3.0:1.0 respectively.

Guilmette Transition Ore Zone

Mantos within either brown-green andradite-wollastonite-vesuvianite-thalite skarns after shaly-silty Dgt or within the silicified marble breccia at the top of Dgs. The mineralogy consists of pyrite, sphalerite, chalcopyrite, galena, tetrahedrite, and chalcocite with lesser amounts of enargite, cuprite II, pyrrhotite, hematite, covellite, and marcasite. Assayed metal ratios for Ag (oz): Pb (oz): Zn (oz): Cu (oz): Mo (oz) are 0.8:0.1:1.8:1.0.

Porphyry and/or the zone consisting of massive brown amphibole, green diopside, wollastonite, sphalerite, and quartz. The zones occur either within this aureole (PW-67) or at its interface with overlying marble breccia (PW-75) characteristic ore mineralogy is relatively simple consisting of magnetite, pyrrhotite, chalcopyrite, cuprite II, pyrite, hematite, enargite, sphalerite, and wolframite. Assayed metal ratios for Ag (oz): Pb (oz): Zn (oz): Cu (oz): Mo (oz) are 0.5:0.1:0.1:1.0:0.3.

Composite aplite biotite quartz monzonite porphyry, porphyritic biotite quartz monzonite, and "breccia" quartz monzonite porphyry showing weak propylitic to phyllic alteration. Disseminated pyrite and chalcopyrite common. Microfractures and veins contain minor amounts of pyrite, chalcopyrite, molybdenite, sphalerite, and bornite. No significant ore intercepts noted to date.

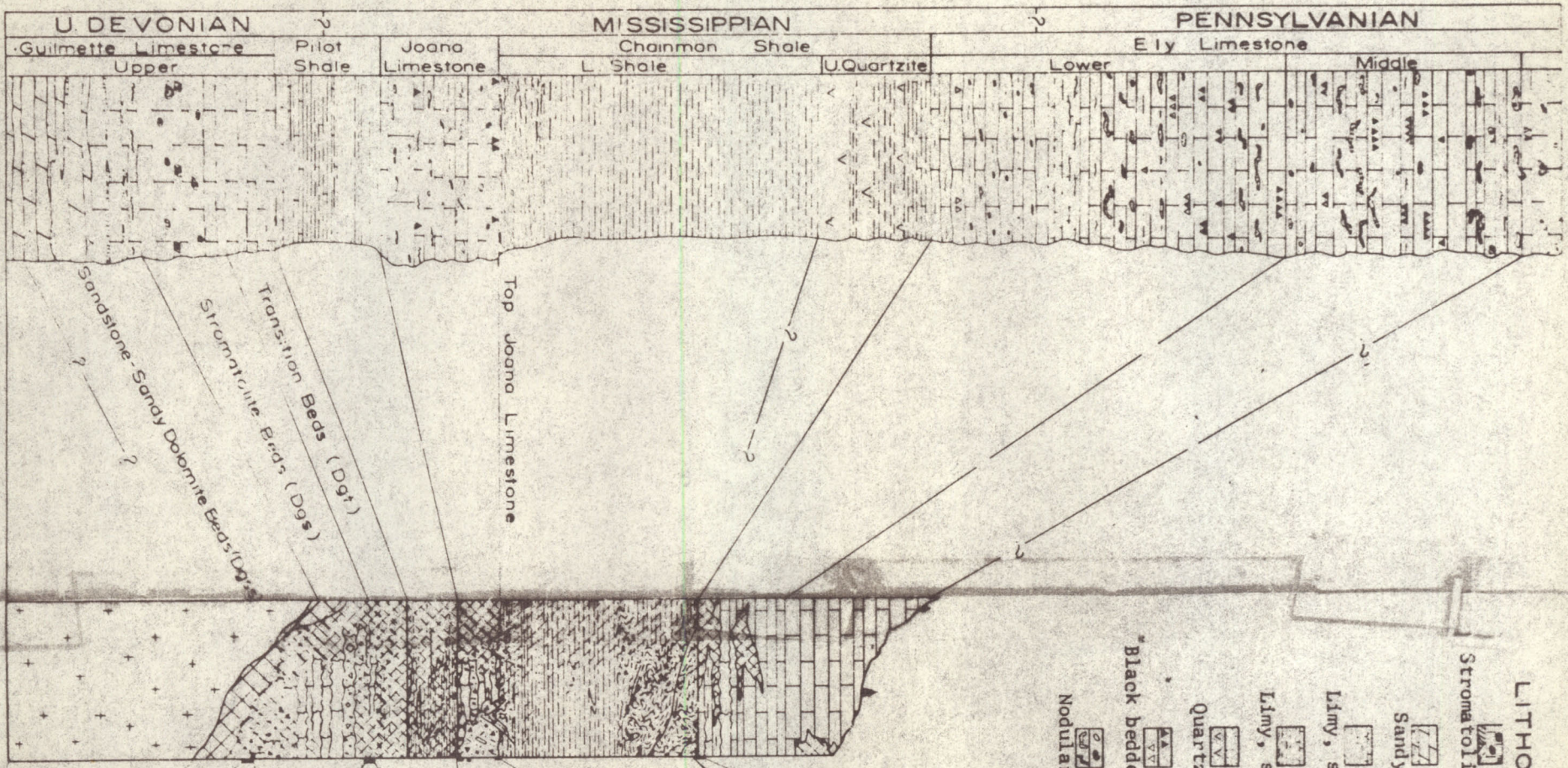
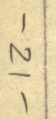
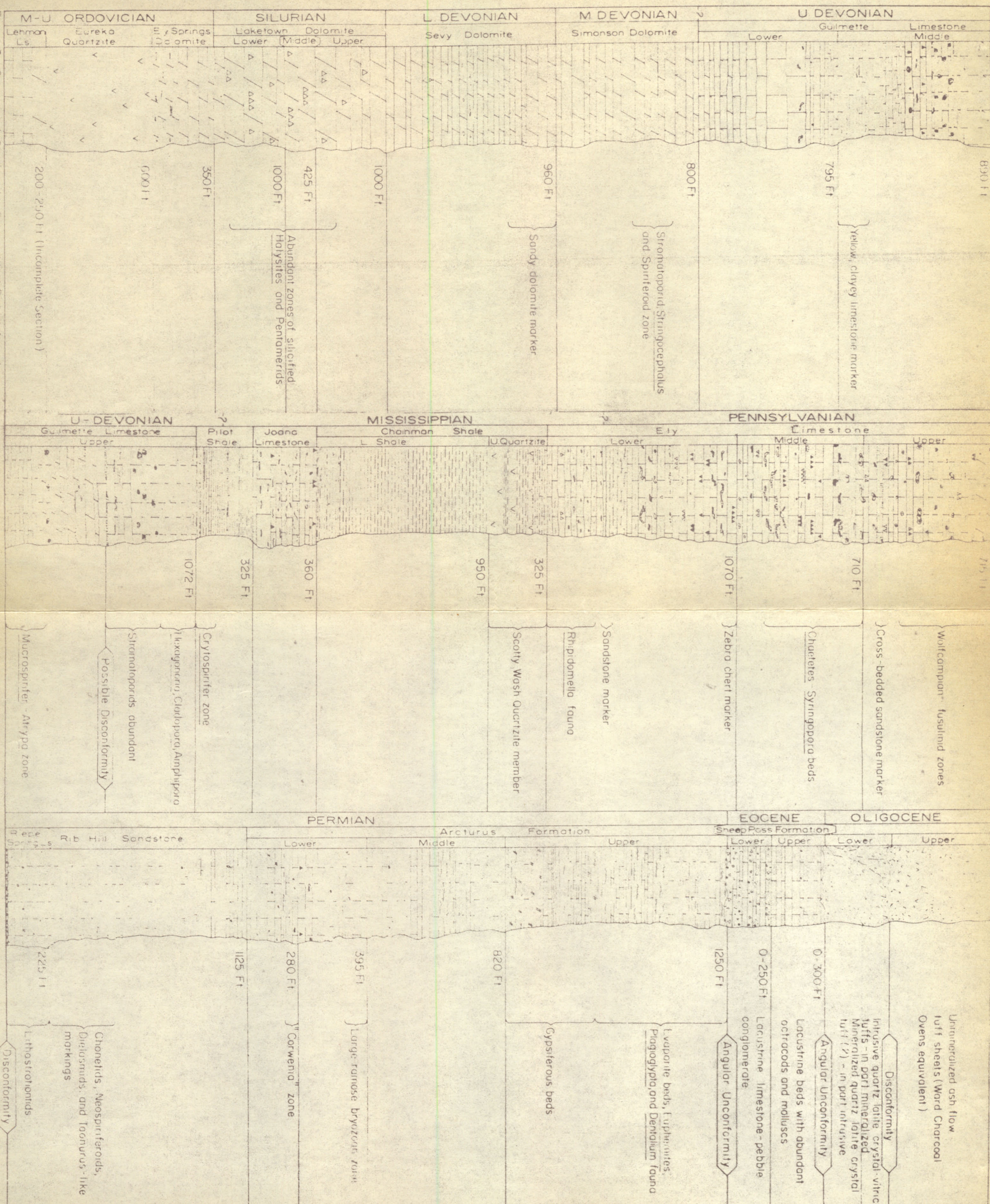


Figure 7. Composite stratigraphic sections showing unaltered and altered-mineralized equivalents, Ward District, Nevada.

5110 0035



5110 0035



5110 0035

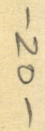




FIGURE 3. Geologic map of the Ward District, White Pine County, Nevada.

Geology by Tom L. Heidrick (1963, 64, '71, '72)

EXPLANATION

STRATIGRAPHY

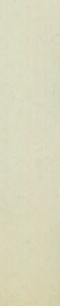
QUATERNARY	Qal	Alluvium
	Qig	Terrace and alluvial fan deposits
	Qdf	Debris flow
	Qde	Debris and earthflows and.
	Qog	Older lacustrine limestone conglomerate and breccia.
OLIGOCENE	Tvi	Unmineralized ash flow tuff
	Tit	Intrusive quartz latite crystal - vitric tuffs
	Tva	Mineralized ash flow tuff
	Tvt	Mineralized quartz latite crystal - lithic tuff (?) in part intrusive
	Tibx	Quartz latite intrusive breccia
Eocene	Ti	Quartz latite and rhyolite porphyry dikes and.
	Tsp ₂	ANGULAR UNCONFORMITY
	Tsp ₁	Sheep Pass lacustrine limestone
	Tsp ₁	Sheep Pass Limestone - pebble conglomerate
	Tsp ₁	ANGULAR UNCONFORMITY
PERMIAN	Pau	Upper Member
	Pam	Arcturus Formation
	Pal	Middle Member
	Pal	Lower Member
	Prh	Rib Hill Sandstone
PENNSYLVANIAN	Prs	Riepe Springs Limestone
	Prs	DISCONFORMITY
	Peu	Upper Member
	Pem	Ely Limestone
	Pei	Middle Member
MISSISSIPPIAN	Mc	Chairman Shale
	MDp	Pilot Shale
	Mja	Joana Limestone
	Mj	amealled and, or unannealed
	Mj	
DEVONIAN	Dgu	Upper Member
	Dgm	Guilmette Limestone
	Dgl	Middle Member
	Dgl	Lower Member
	Ds ₁	Simonson Dolomite
SILURIAN	Ds	Sevy Dolomite
	Slu	Upper Member
	Slm	Laketown Dolomite
	Slm	Middle Member
	SII	Lower Member
ORDOVICIAN	Oes	Ely Springs Dolomite
	Oe	Eureka Quartzite
	Oe	
	OI	Lehman Formation
	OI	

STRUCTURE (Abbrev.)

77	Contact
63 73	Showing direction of dip
U	Fault (und.)
U, D	Showing bearing of dip and slickensides; U, upthrown side, D, downthrown side
28	Thrust fault
57	Showing bearing of dip, sawteeth on hanging wall
42 52	Reverse fault
60	Showing bearing of dip, reversed sawteeth on upthrown hanging wall
60	Normal fault
60	Showing bearing of dip and slickensides, hachures on downthrown side
60	Fault-dike
60	Showing bearing of dip
66 73	Basal glide plane
66 73	Restricted to landslide deposits (Qls)
66 73	Fracture-filling
66 73	Showing bearing of dip and slickensides; c, calcite; cbx, calcite breccia; q, quartz; cqb, calcite-quartz breccia; j, jasperoid und; jc, cherty jasperoid; jl, limonitic jasperoid; jcu, cherty jasperoid showing quartz crackle breccia; jcc, cherty jasperoid showing calcite crackle breccia
45	Anticline
45	Showing trace of axial plane with bearing and plunge of axis and dip of axial plane
45	Syncline
45	See anticline explanation
45 35	Overturned anticline
45 35	Showing trace of axial plane and direction of dips of limbs. Bearing of axis and dip of axial plane as in anticline explanation
45 35	Overturned syncline
45 35	See overturned anticline explanation
45 35	Faulted overturned axial plane
45 35	Showing hachures on downthrown side
45 35	Faulted overturned axial plane
45 35	Showing sawteeth on hanging wall of thrust fault
45 35	Bearing and plunge of axis for minor syncline, anticline and chevron fold
45 35	Dip and strike of upright, horizontal, vertical and overturned beds
45 35	Strike and dip of foliation and plunge of lineation
45 35	Strike of vertical foliation

SILVER KING MINES, Inc.

1000 0 1000 2000 3000 Feet



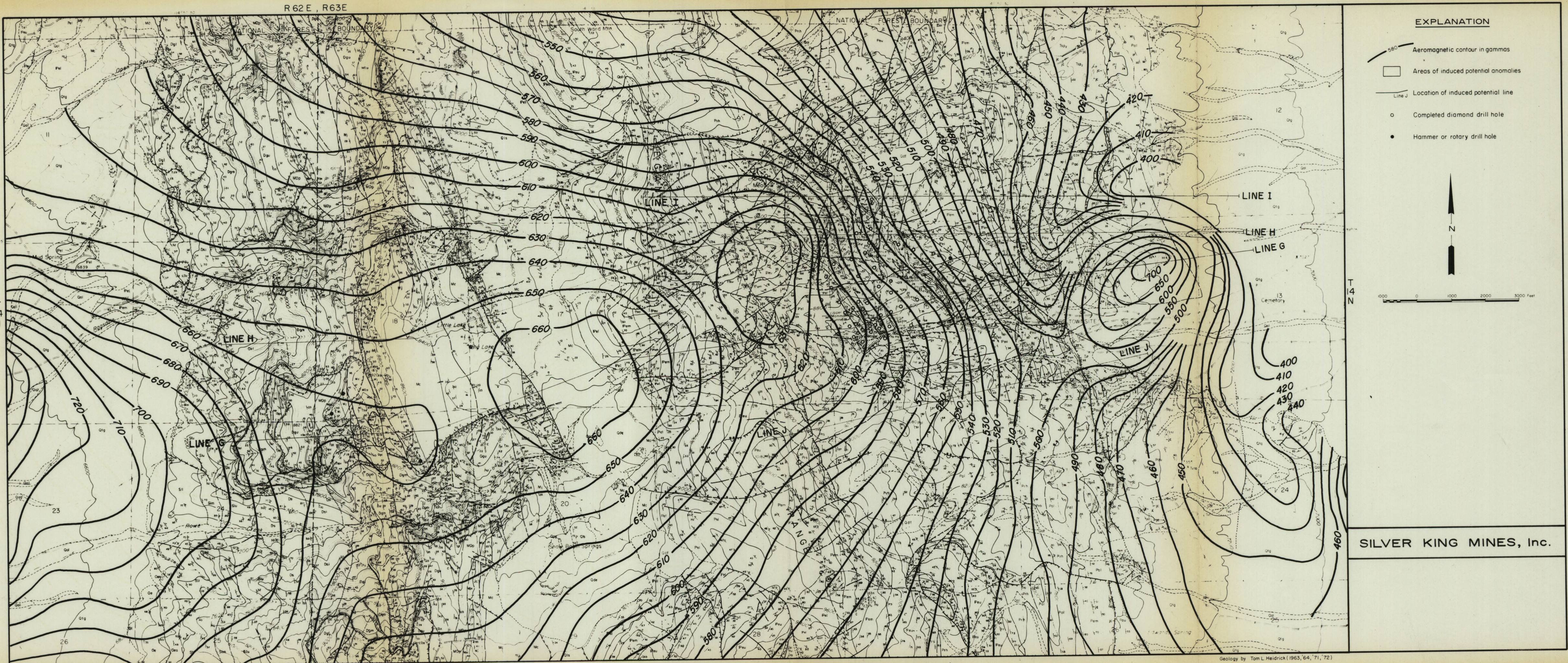


FIGURE 4. Geologic map, low level aeromagnetic map, areas of anomalous induced potential -metal factor and drill hole locations, Ward District, Nevada. See Fig. 3 for geologic map explanation.

Geology by Tom L. Heidrick (1963, '64, '71, '72)

SILVER KING MINES, Inc.

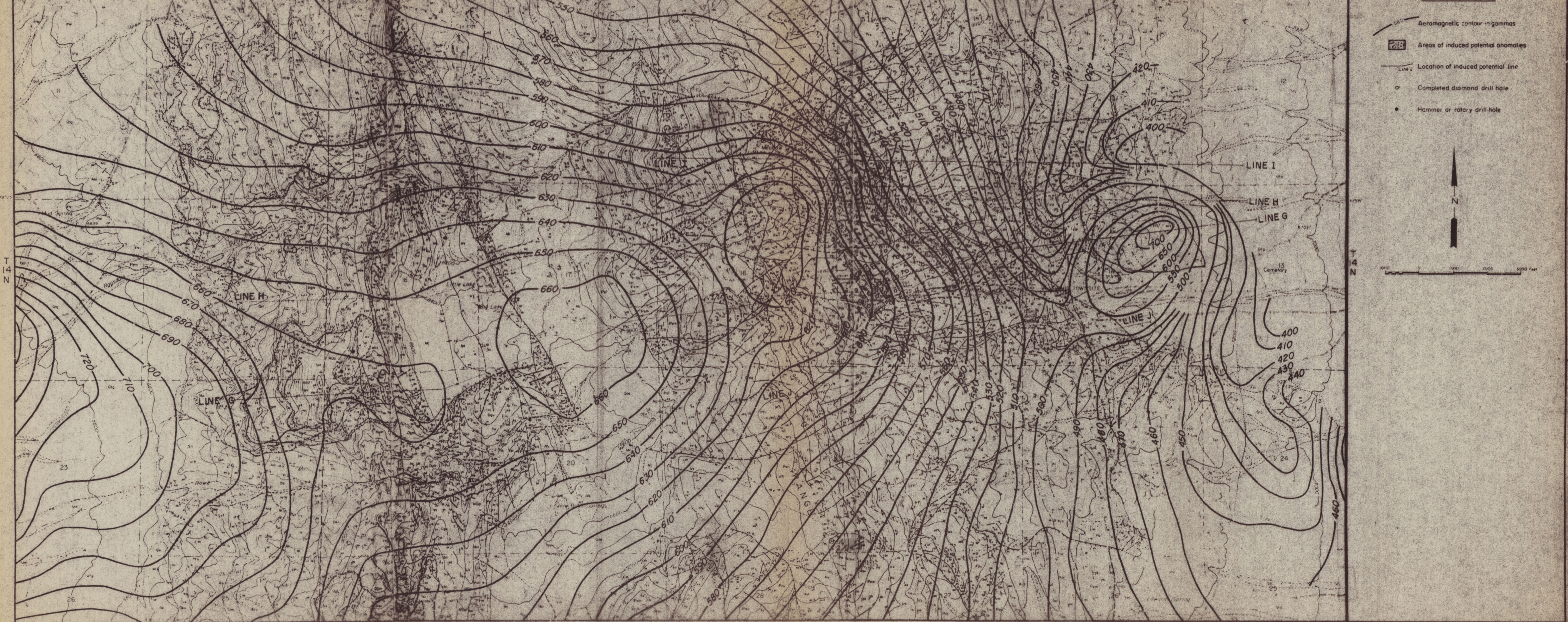


FIGURE 10. Geologic map, low level aeromagnetic map, areas of anomalous induced potential -metal factor and drill hole locations, Ward District, Nevada. See Fig. 3 for geologic map explanation.

Geology by Tom L. Hedrick 1963, 64, p. 12



FIGURE II. Geologic map of the Ward District showing the geochemical distribution of copper contoured in ppm. Data adapted from Brokaw, et al, 1962 and Heidrick, 1965. See Fig. 3 for geologic map explanation.

Geology by Tom L. Heidrick (1963, '64, '71, '72)

Fig 11

2 copies

-39-

5110 0035

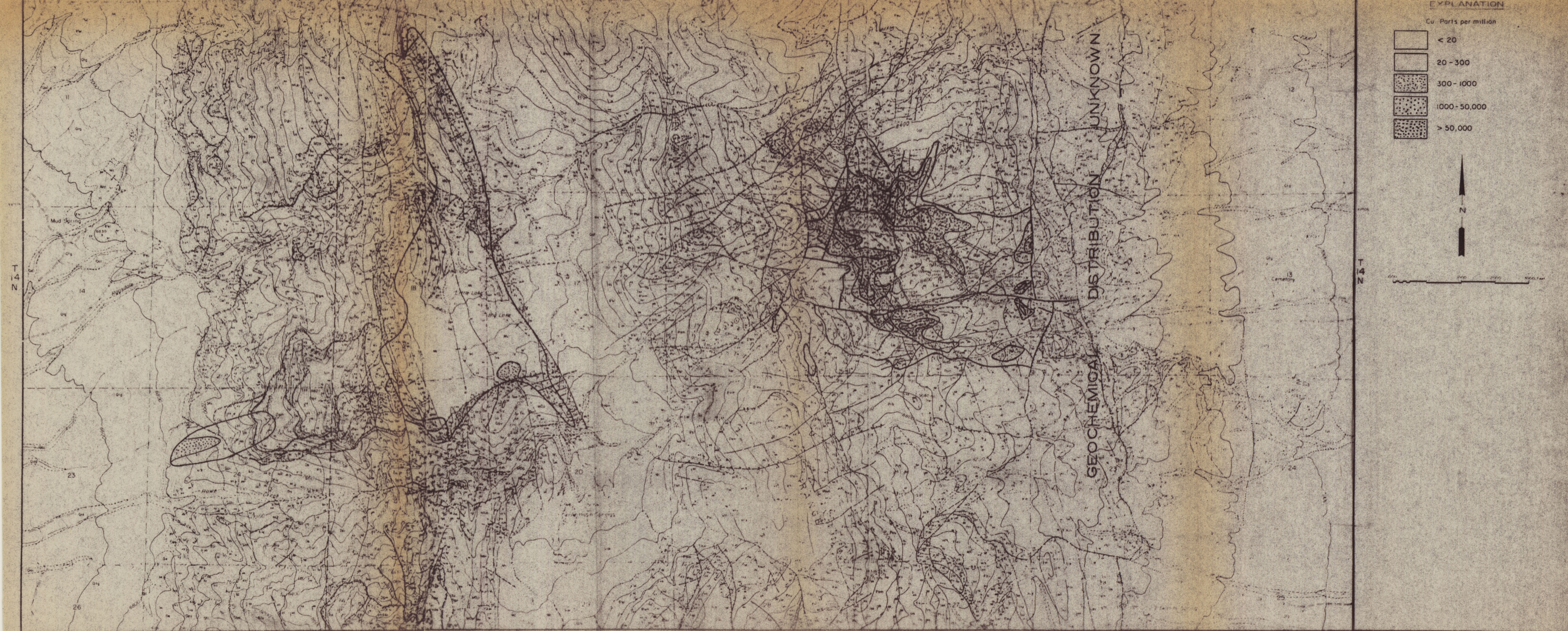


FIGURE II. Geologic map of the Ward District showing the geochemical distribution of copper contoured in ppm. Data obtained from Burton et al. 1952 and Unpublished 1955. See Fig. 3 for geologic map orientation.

5110 0035